Available online at www.sciencedirect.com
SCIENCE DIRECT®
Journal of Organometallic Chemistry 677 (2003) 89–95
Journal of Organometallic Chemistry
www.elsevier.com/locate/jorganchem

Structural studies of lanthanide and yttrium metallocene oxides

William J. Evans *, Benjamin L. Davis, Gregory W. Nyce, Jeremy M. Perotti, Joseph W. Ziller

Department of Chemistry, University of California at Irvine, 516 Rowland Hall, Irvine, CA 92697-2025 USA

Received 6 September 2002; received in revised form 11 April 2003; accepted 14 April 2003

Abstract

Examination of the chemistry of sterically crowded $(C_5Me_4R)_3Ln$ complexes has provided access to a series of $[(C_5Me_4R)_2Ln]_2(\mu$-O) complexes: $[(C_5Me_5)_2La]_2(\mu$-O), $[(C_5Me_5)_2Nd(NC_5H_4NC_4H_8)]_2(\mu$-O), $[(C_5Me_4^iPr)_2Sm]_2(\mu$-O), $[(C_5Me_4Et)_2Gd]_2(\mu$-O), and $[(C_5Me_5)_2Sm(NC_5H_5)]_2(\mu$-O). X-ray crystallographic data on these complexes provide information on the effect of metal and cyclopentadienyl ring size on Ln–O bond distances and Ln–O–Ln angles, which vary between 173 and 180° in these complexes.

Keywords: Cyclopentadienyl; Metallocene; Oxide; Lanthanides

1. Introduction

A consequence of the highly electropositive and oxophilic nature of the lanthanide metals is that organometallic derivatives of these metals frequently react with oxygen-containing compounds to make oxide derivatives. For most types of organometallic complexes, it is difficult to isolate and characterize molecular products from these reactions: either insoluble intractable intermediates are formed or the completely oxidized Ln_2O_3 products result. Hence, little is known about this common type of reaction product.

One class of organometallic compounds that provides isolable oxides is the peralkylmetallocene complexes which contain a $(C_5Me_4R)_2Ln$ unit. Early studies of divalent $(C_5Me_5)_2Sm(THF)_x$ $(x = 1–2)$ [1,2] showed that the oxides $[(C_5Me_5)_2Sm]_2(\mu$-O) [3] and $[(C_5Me_5)_2Sm(THF)]_2(\mu$-O) [4] were readily formed. $[(C_5Me_5)_2Sm]_2(\mu$-O) was structurally characterized and found to have a rather short 2.094 (1) Å Sm–O distance as well as a linear Sm–O–Sm angle. This angle could be explained as a consequence of the necessary close packing of the four large C_5Me_5 rings around the compact Sm–O–Sm core: the four C_5Me_5 ring centroids describe the sterically preferable tetrahedral four coordinate geometry [5].

Since the report of the structure of $[(C_5Me_5)_2Sm]_2(\mu$-O), eight other lanthanide metallocene oxide structures have appeared in the literature: $[(C_5Me_5)_2Ce(THF)]_2(\mu$-O) [6], $[(C_5Me_5)_2Nd]_2(\mu$-O) [7], $[(C_5H_5)_2Yb(OPR_3)]_2(\mu$-O) [8], $[(C_5H_4Me)_2Yb(THF)]_2(\mu$-O) [9], $[(C_5H_5)_2$-$Lu(THF)]_2(\mu$-O) [10], $[(C_9H_7)_2Sm(THF)]_2(\mu$-O) [11], $[(C_5Me_5)_2Sm(CN^tBu)]_2(\mu$-O) [12], and $[(C_5Me_5)_2Y]_2(\mu$-O) [13]. Recently, as part of our effort to make the sterically crowded tris(peralkylcyclopentadienyl) metal complexes, $(C_5R_5)_3Ln$ [14–17], we have isolated several additional examples of metallocene oxides. These have become accessible due to the high reactivity of the $(C_5R_5)_3Ln$ complexes [18–20]. We report here the structures of these complexes and examine their structural features as a function of ligand and metal sizes in comparison with the known examples in the literature.

2. Results and discussion

2.1. Synthesis of $[(C_5Me_4R)_2Ln]_2O$ complexes

Each of the oxides reported here was isolated as a by-product of a reaction or a crystallization conducted under inert atmosphere with starting materials that were thought to be oxygen free. In each case, the high

* Corresponding author. Tel.: +1-949-824-5174; fax: +1-949-824-2210.
E-mail address: wevans@uci.edu (W.J. Evans).

0022-328X/03/$ - see front matter
doi:10.1016/S0022-328X(03)00378-4

reactivity of the reagents led to the formation of oxide bridged bimetallic complexes from trace oxygen sources. Oxygen functionality in the glassware may be responsible in some cases since manipulation of the precursors in silylated glassware reduced the amount of oxide formed.

2.2. X-ray crystallographic data

The X-ray crystal structures of $[(C_5Me_5)_2La]_2(\mu\text{-}O)$ (**1**), $[(C_5Me_4Et)_2Gd]_2(\mu\text{-}O)$ (**2**), $[(C_5Me_4^iPr)_2Sm]_2(\mu\text{-}O)$ (**3**), $[(C_5Me_5)_2Nd(NC_5H_4NC_4H_8)]_2(\mu\text{-}O)$ (**4**), and $[(C_5Me_5)_2Sm(NC_5H_5)]_2(\mu\text{-}O)$ (**5**), are shown in Figs. 1–5. Crystallographic cell parameters are provided in Table 1 and a compilation of bond distances and angles is given in Table 2.

Complexes **1** is isomorphous with the previously reported $[(C_5Me_5)_2Sm]_2(\mu\text{-}O)$ [3]. It contains two symmetry equivalent $(C_5Me_5)_2Ln$ bent metallocene subunits connected via a 180° Ln–O–Ln linkage. The (C_5Me_5 ring centroid)–Ln–(C_5Me_5 ring centroid) angles and Ln–C(C_5Me_5) distance are typical for lanthanum [21].

Complexes **2** and **3** contain C_5Me_4R cyclopentadienyl ligands with substitution greater than that in C_5Me_5. The Ln–O–Ln angles for **2** and **3** are 173.64 (17)° and 177.06 (16)°, respectively. Hence the larger ligands, which lack fivefold symmetry, generate complexes whose structures deviate from the most compact linear Ln–O–Ln arrangement.

The base adducts **4** and **5** are similar to the substituted C_5Me_4R complexes in that an exactly linear Ln–O–Ln arrangement is not observed. Complex **4** has a 174.37 (12)° Nd–O–Nd angle, and complex **5** has a 173.42 (15)° Sm–O–Sm angle. By comparison, the THF adduct $[(C_5Me_5)_2Ce(THF)]_2(\mu\text{-}O)$ [6] has a Ce–O–Ce angle of 175.9°, and the isonitrile adduct $[(C_5Me_5)_2Sm(CN^t\text{-}Bu)]_2(\mu\text{-}O)$ [12] has a Sm–O–Sm angle of 174.3°.

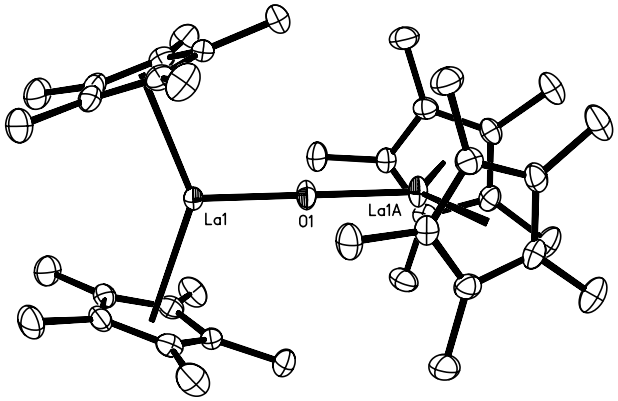

Fig. 1. Thermal ellipsoid plot of $[(C_5Me_5)_2La]_2(\mu\text{-}O)$ (**1**), with thermal ellipsoids drawn at the 50% probability level. Hydrogen atoms are omitted for clarity.

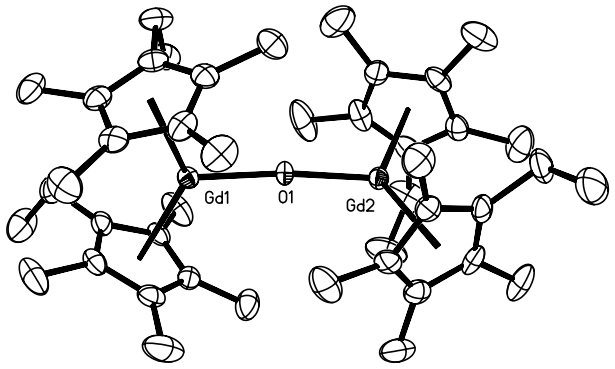

Fig. 2. Thermal ellipsoid plot of $[(C_5Me_4Et)_2Gd]_2(\mu\text{-}O)$ (**2**), with thermal ellipsoids drawn at the 50% probability level. Hydrogen atoms are omitted for clarity.

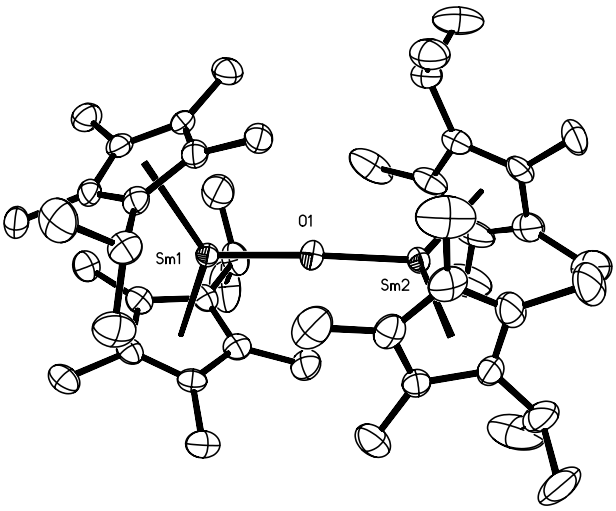

Fig. 3. Thermal ellipsoid plot of $[(C_5Me_4^iPr)_2Sm]_2(\mu\text{-}O)$ (**3**), with thermal ellipsoids drawn at the 50% probability level. Hydrogen atoms are omitted for clarity.

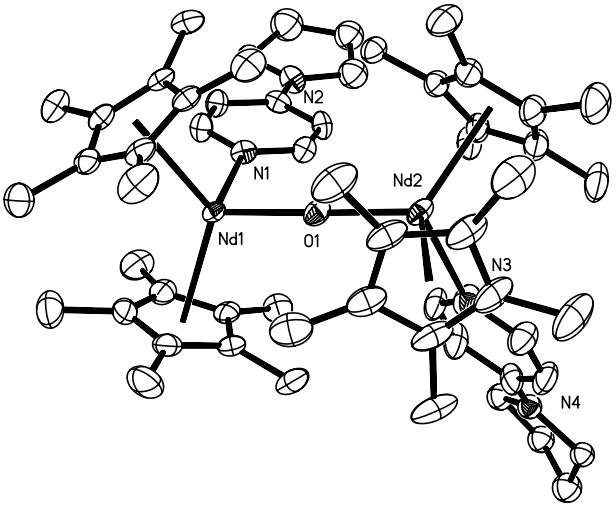

Fig. 4. Thermal ellipsoid plot of $[(C_5Me_5)_2Nd(NC_5H_4NC_4H_8)]_2(\mu\text{-}O)$ (**4**), with thermal ellipsoids drawn at the 50% probability level. Hydrogen atoms are omitted for clarity.

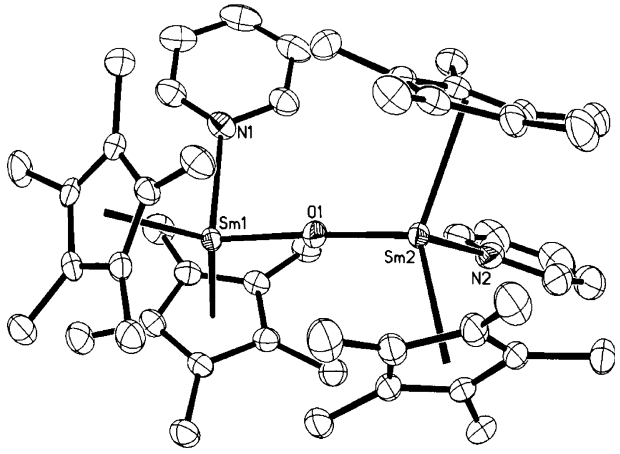

Fig. 5. Thermal ellipsoid plot of $[(C_5Me_5)_2Nd(NC_5H_5)]_2(\mu\text{-}O)$ (**5**), with thermal ellipsoids drawn at the 50% probability level. Hydrogen atoms are omitted for clarity.

2.3. Correlation between Ln–O bond distance and metal radius

Fig. 6 shows a plot of the Ln–O bond distances for all lanthanide metallocene oxide structures characterized to date as a function of the metal radius adjusted for **7** or **8** coordination using the data of Shannon [22]. The most extensive single series of complexes belongs to the $[(C_5Me_5)_2Ln]_2(\mu\text{-}O)$ complexes; the four entries form a line with $R^2 = 0.899$. This means that the short 2.094 (1) Å Sm–O distance observed for $[(C_5Me_5)_2Sm]_2(\mu\text{-}O)$ is not unusual for this class of complexes. Each member of the $[(C_5Me_5)_2Ln]_2(\mu\text{-}O)$ series has comparably short Ln–O distances. The recent X-ray crystal structure of $[([Me_3Si]_2N)_2(THF)Sm]_2(\mu\text{-}O)$ has a similar short Sm–O distance, 2.0819(2) Å and a 180° Sm–O–Sm angle [23].

The other entries can be discussed in three groups. The first group, the base adduct complexes, $[(C_5Me_5)_2LnL]_2(\mu\text{-}O)$, are located at the right upper corner of the graph. This is reasonable since these higher coordinate complexes have larger metal radii and would be expected to have longer Ln–O distances [22]. These complexes are found both above and below the $[(C_5Me_5)_2Ln]_2(\mu\text{-}O)$ line, but do not deviate greatly from the line. Hence, there is a reasonable correlation between the metal oxygen distance and the coordination number adjusted radius ($R^2 = 0.874$).

A second group of oxides is comprised of the C_5Me_4R complexes $[(C_5Me_4Et)_2Gd]_2(\mu\text{-}O)$ and $[(C_5Me_4^iPr)_2Sm]_2(\mu\text{-}O)$. Their Ln–O values fall above the $[(C_5Me_5)_2Ln]_2(\mu\text{-}O)$ line, i.e. they have longer Ln–O distances. This is reasonable since these complexes are more sterically crowded.

The third group involves metallocenes not as highly substituted as C_5Me_5. These all lie below the $[(C_5Me_5)_2Ln]_2(\mu\text{-}O)$ line, i.e. they have smaller Ln–O distances, as might be expected for the less sterically bulky systems. If a separate line were drawn using these data, it would be roughly parallel with the $[(C_5Me_5)_2Ln]_2(\mu\text{-}O)$ line. However, more metal complexes are needed for a reliable correlation.

2.4. Ln–O–Ln variations

In contrast to the Ln–O data, the Ln–O–Ln angles do not vary regularly as a function of either the Ln–O

Table 1
X-ray data collection parameters for $[(C_5Me_5)_2La]_2(\mu\text{-}O)$ (**1**), $[(C_5Me_4Et)_2Gd]_2(\mu\text{-}O)$ (**2**), $[(C_5Me_4^iPr)_2Sm]_2(\mu\text{-}O)$ (**3**), $[(C_5Me_5)_2Nd(NC_5H_4NC_4H_8)]_2(\mu\text{-}O)$ (**4**), and $[(C_5Me_5)_2Sm(NC_5H_5)]_2(\mu\text{-}O)$ (**5**)

	1	**2**	**3**	**4**	**5**
Formula	$C_{40}H_{60}La_2O$	$C_{44}H_{68}Gd_2O$	$C_{48}H_{76}OSm_2$	$C_{58}H_{76}N_4Nd_2O\cdot 2(C_6H_6)$	$C_{50}H_{70}N_2Sm_2O\cdot(C_7H_8)$
Formula weight	834.70	927.48	969.79	1289.92	1107.91
Space group	$I\bar{4}2m$	$P\bar{1}$	$P\bar{1}$	$P\bar{1}$	$P2_12_12_1$
Crystal system	tetragonal	triclinic	triclinic	triclinic	orthorhombic
a (Å)	11.4933 (4)	10.8110 (4)	9.9057 (3)	14.6640 (7)	10.8812 (4)
b (Å)		11.4623 (4)	13.9230 (5)	15.0935 (7)	14.1308 (5)
c (Å)	14.2351 (6)	17.5122 (6)	17.9850 (6)	16.5376 (8)	33.0478 (11)
α (°)		87.8680 (10)	76.2730 (10)	86.6970 (10)	
β (°)		72.2480 (10)	76.8650 (10)	66.9300 (10)	
γ (°)		80.0360 (10)	72.3600 (10)	72.9250 (10)	
V (Å^3)	1880.40 (12)	2035.31 (12)	2263.73 (13)	3212.3 (3)	5081.4 (3)
Z	2	2	2	2	4
λ (Å)	0.71073	0.71073	0.71073	0.71073	0.71073
ρ_{calc} (Mg m^{-3})	1.474	1.513	1.423	1.334	1.448
μ (Mo–K$_\alpha$) (mm^{-1})	2.269	3.261	2.600	1.642	2.328
Temperature (K)	158	158	163	158	163
R [a] ($I > 2\sigma(I)$): R_1	0.0156	0.0362	0.0380	0.0354	0.0251
R [b] (all data): wR_2	0.0390	0.0886	0.0884	0.0942	0.0661

[a] $R_1 = \Sigma||F_o| - |F_c||/\Sigma|F_o|$.
[b] $wR_2 = [\Sigma[w(F_o^2 - F_c^2)^2]/\Sigma(w(F_o^2)^2)]^{1/2}$.

Table 2
Selected bond distances and angles for $[(C_5Me_5)_2La]_2(\mu\text{-}O)$ (**1**), $[(C_5Me_4Et)_2Gd]_2(\mu\text{-}O)$ (**2**), $[(C_5Me_4^iPr)_2Sm]_2(\mu\text{-}O)$ (**3**), $[(C_5Me_5)_2Nd(NC_5H_4NC_4H_8)]_2(\mu\text{-}O)$ (**4**), and $[(C_5Me_5)_2Sm(NC_5H_5)]_2(\mu\text{-}O)$ (**5**)

Compound	Ln–C_5R_5 ring centroid distance (Å)	Ln–C(C_5R_5 ring) average distance (Å)	Ln–C(C_5R_5 ring) range of distances (Å)	C_5R_5 ring centroid-metal-C_5R_5 ring centroid angle (°)	Ln–O–Ln angle (°)	Ln–O distance (Å)	Ln–Lewis Base distance (Å)
$[(C_5Me_5)_2La]_2(\mu\text{-}O)$ (**1**)	2.561	2.82	2.811–2.852	139.8	180.0	2.1443(3)	n/a
$[(C_5Me_4Et)_2Gd]_2(\mu\text{-}O)$ (**2**)	2.443 2.446	2.72	2.681–2.781	134.4, 133.8	173.64(17)	2.118(3)	n/a
$[(C_5Me_4^iPr)_2Sm]_2(\mu\text{-}O)$ (**3**)	2.462 2.465 2.470 2.471	2.74	2.709–2.798	136.4, 134.3	177.06(16)	2.116(3)	n/a
$[(C_5Me_5)_2Nd(NC_5H_4NC_4H_8)]_2(\mu\text{-}O)$ (**4**)	2.574 2.579 2.582 2.584	2.84	2.794–2.904	129.4, 129.1	174.37(12)	2.157(2)	2.554(3)
$[(C_5Me_5)_2Sm(NC_5H_5)]_2(\mu\text{-}O)$ (**5**)	2.534 2.537 2.535 2.542	2.81	2.742–2.882	128.3, 128.9	173.42(15)	2.151(2)	2.576(3)

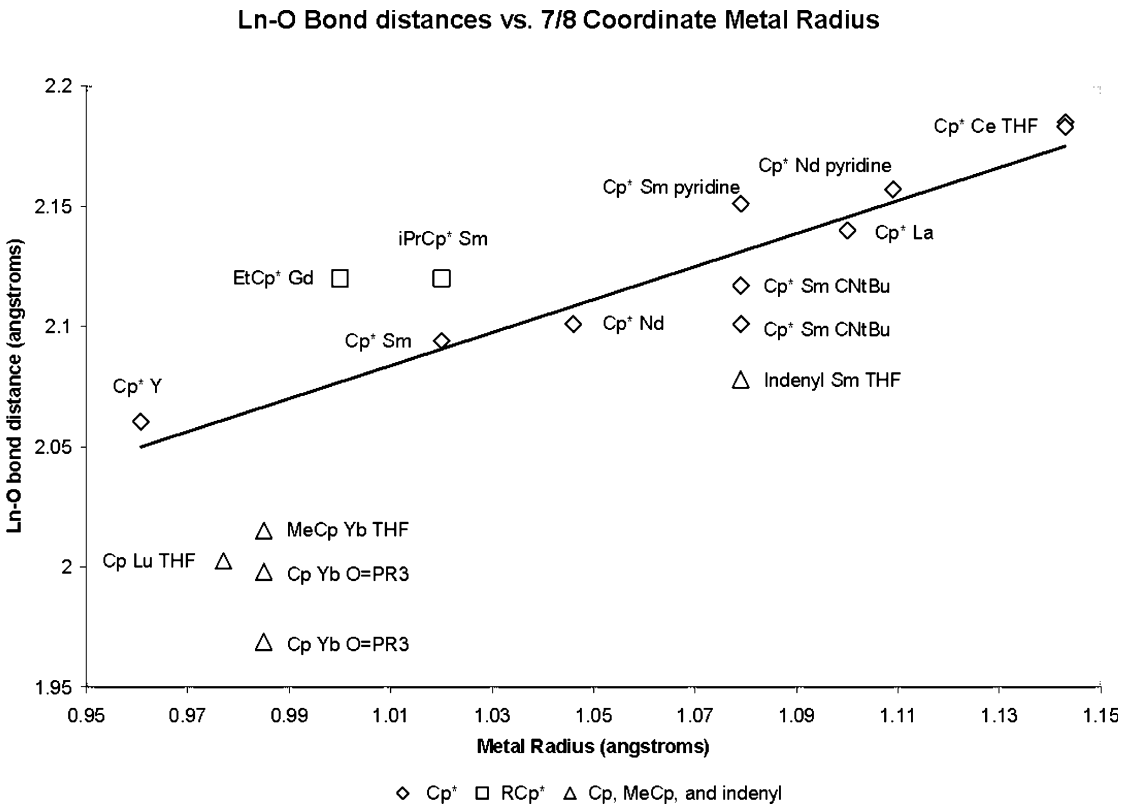

Fig. 6. Ln–O bond distance vs. 7/8 coordinate metal radius for [(cyclopentadienyl)$_2$lanthanide]$_2$(μ-O)] and [(cyclopentadienyl)$_2$lanthanide(base)]$_2$(μ-O)] complexes. Symbols are identified by identity of the ring, the metal, and the base if any.

distance or the metal radius. It has been previously observed for metal alkoxides of electropositive metals that there is not a strong correlation between M–O distance and M–O–C angle [24,25]. The M–O and M–O–M data here are similar. The variation in M–O–M angles is also consistent with the shallow energy potentials calculated for changing angles in lanthanide complexes [26].

The complexes which deviate from 180° M–O–M angles are those that are asymmetric, either by having a base adduct or by having a cyclopentadienyl ring with less than C_5 symmetry. These non-linear deviations may occur to optimize the packing of the asymmetrical components. In a system in which there are not strong orbital factors influencing the M–O–M angle potential, this presumably gives a more stable structure.

3. Conclusion

In summary, the Ln–O distances in [(cyclopentadienyl)$_2$lanthanide]$_2$(μ-O)] and [(cyclopentadienyl)$_2$lanthanide(base)]$_2$(μ-O)] complexes seem to correlate reasonably well with metal size and ligand bulk as might be expected. The Ln–O–Ln angles are more variable and depend on the symmetry/asymmetry of the system.

4. Experimental

4.1. Synthesis

Crystals of **1**–**3** were obtained from attempted syntheses of $(C_5Me_4R)_3Ln$ complexes, from $(C_5Me_4R)_2LnBPh_4$ and KC_5Me_4R [17]. In each case, the crystals were the dominant product. Light yellow crystals of [$(C_5Me_5)_2La]_2$(μ-O) (^{1}H-NMR: 2.03 ppm), **1**, were obtained while attempting to crystallize $(C_5Me_5)_3La$ [27] from hot toluene in a glass vial. Yellow crystals of [$(C_5Me_4Et)_2Gd]_2$(μ-O) (**2**) were obtained while attempting to crystallize $(C_5Me_4Et)_3Gd$ from hot toluene in a glass vial. Yellow crystals of [$(C_5Me_4^iPr)_2Sm]_2$(μ-O) (**3**) were obtained while attempting to crystallize $(C_5Me_4^iPr)_3Sm$ from hot toluene in a glass vial. Light blue crystals of [$(C_5Me_5)_2$Nd-$(NC_5H_4NC_4H_8)]_2$(μ-O) (**4**) were obtained by reacting $(C_5Me_5)_3Nd$ [17] with $NC_5H_4NC_4H_8$. Orange crystals of [$(C_5Me_5)_2Sm(NC_5H_5)]_2$(μ-O) (**5**) were obtained from the reaction of $(C_5Me_5)_3Sm$ [14] and pyridine.

4.2. X-ray data collection, structure determination, and refinement for the $[(C_5Me_5)_2Ln]_2(\mu\text{-}O)$ complexes 1–5

In all cases, a crystal of dimensions reported in Table 1 was mounted on a glass fiber and transferred to a Bruker/Siemens P4 diffractometer (Complex **1**) or Bruker CCD platform diffractometer (Complex **2**–**5**). For complex **1**, the XSCANS [28] program package was used to determine the Laue symmetry, crystal class, unit-cell parameters and for data collection. Intensity data were collected at 158 K using a $2\theta/\omega$ scan technique with Mo–K_α radiation. The raw data were processed with a local version of CARESS [29] which employs a modified version of the Lehman–Larsen algorithm to obtain intensities and standard deviations from the measured 96-step profiles. For the complexes **2**–**5**, the SMART [30] program package was used to determine the unit-cell parameters and for data collection. A 20 s frame^{-1} scan time for a sphere of diffraction data was collected on complexes **3**–**5**, and a 30 s frame^{-1} scan time for a sphere of data on complex **2**. The raw frame data [31]was processed using SAINT [32] and SADABS [31] to yield the reflection data file. For all complexes, subsequent calculations were carried out using the SHELXTL [31] program. The structures were solved by direct methods and refined on F^2 by full-matrix least-squares techniques. The analytical scattering factors [33] for neutral atoms were used throughout the analysis. Hydrogen atoms were located from a difference-Fourier map and refined (x, y, z and U_{iso}) or were included using a riding model.

4.2.1. $[(C_5Me_5)_2La]_2O$ (1)

All data were corrected for absorption and for Lorentz and polarization effects and placed on an approximately absolute scale. The Laue group was 4/*mmm* and the systematic absences were consistent with space group $I\bar{4}2m$ which was later determined to be correct. The molecule was located on a site of $\bar{4}2m$ symmetry. At convergence, $wR_2 = 0.0390$ and GOF = 1.177 for 59 variables refined against 692 data. As a comparison for refinement on F, $R_1 = 0.0156$ for those 665 data with $I > 2.0\sigma(I)$. The absolute structure was assigned by refinement of the Flack parameter [34].

4.2.2. $[(C_5Me_4Et)_2Gd]_2O$ (2)

There were neither systematic absences nor any diffraction symmetry other than the Friedel condition. The centrosymmetric triclinic space group $P\bar{1}$ was assigned and later determined to be correct. At convergence, $wR_2 = 0.0886$ and GOF = 1.058 for 424 variables refined against 9664 data. As a comparison for refinement on F, $R_1 = 0.0362$ for those 7650 data with $I > 2.0\sigma(I)$.

4.2.3. $[(C_5Me_4^iPr)_2Sm]_2O$ (3)

There were neither systematic absences nor any diffraction symmetry other than the Friedel condition. The centrosymmetric triclinic space group $P\bar{1}$ was assigned and later determined to be correct. At convergence, $wR_2 = 0.0884$ and GOF = 1.041 for 460 variables refined against 10 691 data (as a comparison for refinement on F, $R_1 = 0.0380$ for those 8337 data with $I > 2.0\sigma(I)$).

4.2.4. $[(C_5Me_5)_2Nd(NC_5H_4NC_4H_8)]_2O$ (4)

There were neither systematic absences nor any diffraction symmetry other than the Friedel condition. The centrosymmetric triclinic space group $P\bar{1}$ was assigned and later determined to be correct. The pyrrole rings and benzene solvent molecules were disordered and included using multiple components with partial site-occupancy-factors. The hydrogen atoms associated with the pyrrole rings were not included. At convergence, $wR_2 = 0.0942$ and GOF = 1.028 for 618 variables refined against 15 112 data. As a comparison for refinement on F, $R_1 = 0.0354$ for those 11 657 data with $I > 2.0\sigma(I)$.

4.2.5. $[(C_5Me_5)_2Nd(NC_5H_5)]_2O$ (5)

The diffraction symmetry was *mmm* and the systematic absences were consistent with the orthorhombic space group $P2_12_12_1$ which was later determined to be correct. There was one molecule of toluene solvent present per formula unit. At convergence, $wR_2 = 0.0661$ and GOF = 1.126 for 559 variables refined against 12 411 data. As a comparison for refinement on F, $R_1 = 0.0251$ for those 11 971 data with $I > 2.0\sigma(I)$. The absolute structure was assigned by refinement of the Flack parameter [6].

5. Supplemental material

Crystallographic data for the structural analysis have been deposited with the Cambridge Crystallographic Data Centre, CCDC nos. 207292–207296 for compounds **1**–**5**, respectively. Copies of this information may be obtained free of charge from The Director, CCDC, 12 Union Road, Cambridge, CB2 1EZ UK (Fax: +44-1223-336033; or e-mail: deposit@ccdc.cam.ac.uk; or www: http://www.ccdc.cam.ac.uk).

Acknowledgements

We thank the National Science Foundation for support for this research.

References

[1] W.J. Evans, I. Bloom, W.E. Hunter, J.L. Atwood, J. Am. Chem. Soc. 103 (1981) 6507.
[2] W.J. Evans, L.A. Hughes, T.P. Hanusa, J. Am. Chem. Soc. 106 (1984) 4270.
[3] W.J. Evans, J.W. Grate, I. Bloom, W.E. Hunter, J.L. Atwood, J. Am. Chem. Soc. 107 (1985) 405.
[4] W.J. Evans, S.L. Gonzales, J. Organomet. Chem. 480 (1994) 41.
[5] W.J. Evans, J. Alloys Compounds 192 (1993) 205.
[6] B.J. Deelman, M. Booij, A. Meetsma, J.H. Teuben, H. Kooijman, A.L. Spek, Organometallics 14 (1995) 2306.
[7] D. Tilley, Personal Communication to Cambridge Structure Database, 1996.
[8] G.B. Deacon, G.D. Fallon, C.M. Forsyth, B.M. Gatehouse, P.C. Junk, A. Philosof, P.A. White, J. Organomet. Chem. 565 (1998) 201.
[9] M. Adam, G. Massarweh, R.D. Fischer, J. Organomet. Chem. 405 (1991) C33.
[10] H. Schumann, E. Palamidis, J. Loebel, J. Organomet. Chem. 384 (1990) C49.
[11] W.J. Evans, T.S. Gummersheimer, J.W. Ziller, Appl. Organomet. Chem. 9 (1995) 437.
[12] W.J. Evans, D.K. Drummond, L.A. Hughes, H. Zhang, J.L. Atwood, Polyhedron 7 (1988) 1693.
[13] S.N. Ringelberg, A. Meetsma, S.I. Troyanov, B. Hessen, J.H. Teuben, Organometallics 21 (2002) 1759.
[14] W.J. Evans, S.L. Gonzales, J.W. Ziller, J. Am. Chem. Soc. 113 (1991) 7423.
[15] W.J. Evans, K.J. Forrestal, J.T. Leman, J.W. Ziller, Organometallics 15 (1996) 527.
[16] W.J. Evans, K.J. Forrestal, J.W. Ziller, Angew. Chem. Int. Ed. 36 (1997) 774.
[17] W.J. Evans, C.A. Seibel, J.W. Ziller, J. Am. Chem. Soc. 120 (1998) 6745.
[18] W.J. Evans, K.J. Forrestal, J.W. Ziller, J. Am. Chem. Soc. 117 (1995) 12635.
[19] W.J. Evans, K.J. Forrestal, J.W. Ziller, J. Am. Chem. Soc. 120 (1998) 9273.
[20] W.J. Evans, G.W. Nyce, R.D. Clark, R.J. Doedens, J.W. Ziller, Angew. Chem. Int. Ed. 38 (1999) 1801.
[21] W.J. Evans, S.E. Foster, J. Organomet. Chem. 433 (1992) 79.
[22] R.D. Shannon, Acta Crystallogr. A 32 (1976) 751.
[23] E.D. Brady, D.L. Clark, D. Webster Keogh, B.L. Scott, J.G. Watkin, J. Am. Chem. Soc. 124 (2002) 7007.
[24] W.A. Howard, T.M. Trnka, G. Parkin, Inorg. Chem. 34 (1995) 5900.
[25] B.D. Steffey, P.E. Fanwick, I.P. Rothwell, Polyhedron 9 (1990) 963.
[26] R. Hoffmann, J.V. Ortiz, Inorg. Chem. 24 (1985) 2095.
[27] W.J. Evans, B.L. Davis, J.W. Ziller, Inorg. Chem. 40 (2001) 6341.
[28] XSCANS Software Users Guide, Version 2.1, Siemens Analytical X-Ray Systems, Inc.; Madison, WI 1994.
[29] R.W. Broach, CARESS, Argonne National Laboratory, Illinois, 1978.
[30] SMART Software Users Guide, Version 4.21; Bruker Analytical X-Ray Systems, Inc.; Madison, WI 1997.
[31] G.M. Sheldrick, SHELXTL Version 5.10; Bruker Analytical X-Ray Systems, Inc., Madison,WI, 1997.
[32] SAINT Software Users Guide, Version 4.05; Bruker Analytical X-ray Systems, Inc.; Madison, WI 1997.
[33] International Tables for X-ray Crystallography, Kluwer Academic Publishers; Dordrecht 1992.
[34] H.D. Flack, Acta Crystallogr. A 39 (1983) 876.